Nonlinear two-stage model for color discrimination

Taisuke Inamura,[1] Satoshi Shioiri,[2,*] Sei-ichi Tsujimura,[3] and Hirohisa Yaguchi[1]

[1]*Graduate School of Advanced Integration Science, Chiba University, 1-33 Yayoicho, Inage-ku, Chiba 263-8522, Japan*
[2]*Research Institute of Electrical Communication, Tohoku University, 2-1-1 Katahira, Aoba-ku, Sendai 980-8577, Japan*
[3]*Graduate School of Science and Engineering, Kagoshima University, 1-21-40 Koorimoto, Kagoshima 890-0065, Japan*
**Corresponding author: shioiri@riec.tohoku.ac.jp*

Received June 1, 2010; revised January 30, 2011; accepted February 2, 2011;
posted February 8, 2011 (Doc. ID 129331); published March 31, 2011

We modified a two-stage model for color discrimination proposed in a previous study [Color Res. Appl. **25**, 105 (2000)]; in order to extend the model to wider conditions, we considered the conditions with luminance modulations in addition to color modulations. Using the modified model, we successfully predicted color discrimination data with test color changes along both the chromatic and luminance axes under a variety of background colors. Both qualitative and quantitative assessments in modeling showed that nonlinearity is required in both the cone and the cone-opponent stages to interpret adaptation effects of both color and luminance on color discrimination. This fact suggests that the nonlinear properties at each stage have different roles in color perception.

OCIS codes: 330.1690, 330.1720, 330.4060.

1. INTRODUCTION

The color discrimination characteristics of human vision are important and useful both for understanding human color vision and for developing a uniform color space. Many color scientists have attempted to model the mechanisms of color discrimination based on psychophysical experiments. The line element theory proposed by Helmholtz is one such attempt at explaining the experimental results. The line element theory is based on the trichromatic theory of color vision and Weber's law [1] and is able to predict color discrimination thresholds from different colors covering a wide area in color spaces such as MacAdam's ellipses [2]. Another example is CIE 1976 $L^*a^*b^*$ color space. Distance in CIE 1976 $L^*a^*b^*$ color space is assumed to correspond to the perceptual difference in color and is used as an index of the discriminability of two colors for various kinds of applications. However, these models require complicated mathematical transformations that are not related to physiological processes.

More recent studies have adopted opponent color mechanisms in their models. Boynton *et al.* showed that color discrimination thresholds can be predicted by the responses of color-opponent mechanisms if data are appropriately normalized for each of the red/green and yellow/blue opponent mechanisms [3]. Subsequently, a number of studies confirmed contributions of color-opponent mechanisms to color discrimination in a variety of experimental conditions [4–15].

Moreover, it has also been suggested that nonlinear processes are necessary to predict color discrimination data in a variety of conditions. One of the well-used nonlinearities is logarithm. Logarithmic nonlinearity in color (or intensity) coding predicts Weber's law, and logarithmic transformation is equivalent to express cone outputs in a cone contrast diagram. The relative weights of L- and M-cone systems to the M – L mechanism at threshold is close to unity in the cone contrast space in various background color conditions [10,12,14,16].

Some of the models assume nonlinearity at the opponent color stage (the second, postreceptoral cone-opponent site) as well in the cone process (the first, cone-specific site) to accord with physiological facts [5–7]. Perhaps the model proposed by Smith, Pokorny, and Sun (SPS model) fits best physiologically, because the model's parameters were determined based on observation of the behavior of retinal ganglion cells in macaque retinas. Smith *et al.* [6] showed that this model was able to predict discrimination thresholds measured psychophysically for colors varying along the L – M cone-opponent direction with a fixed luminance.

A question that should be considered next is the effect of varying the luminance with color, which was not considered seriously in Smith *et al.*'s study. We know that adaptation to a light environment changes our color vision drastically. The purpose of this study is to extend Smith *et al.*'s model to a wider variety of conditions, where both luminance and chrominance vary. For this purpose, we used data from Kawamoto *et al.* [17], who measured color discrimination thresholds with different background colors distributed on the LM plane in the cone excitation space. They varied background and test colors along either of four directions on the LM plane and determined discrimination thresholds for each combination of the test and background. The use of various background colors on the LM plane provided information on the adaptation effect due to both luminance and color changes. The use of various test color directions provided information on the change of the contribution ratio of L and M cones to the red–green opponent mechanism [18–22].

Considering these two factors, we modified the model of Smith *et al.* in order to extend the scope of the field covered by the model, and we applied the model to the data of Kawamoto *et al.* We also investigated how nonlinearity at the cone and opponent stages influences prediction performance. Kawamoto *et al.* used a four-spatial alternative forced choice procedure with gradual temporal change in the test to focus on color discrimination properties of the color-opponent

mechanism. Before presenting the model's predictions, we briefly describe the experiment of Kawamoto *et al.* (see [17] for details).

2. EXPERIMENT

A. Apparatus

The test stimuli were generated on a Sony GDM-17SE2T monitor controlled by a Cambridge Research Systems VSG 2/4 graphic card, with 15 bit luminance-calibrated lookup tables. Observations were performed with natural pupils in a dark booth at a viewing distance of 500 mm from the CRT.

B. Stimuli

The experiments were carried out on the LM cone excitation plane. The background color was systematically chosen along one of four directions: L, M, L – M, and L + M in the LM plane centered on equal energy white point (34.5 cd/m^2) with a constant S cone excitation. In the LM plane, L- and M-cone stimulus values were expressed in terms of luminance in cd/m^2 as in Kawamoto *et al.* (the luminance of the color was divided into each cone stimulus value based on the activity ratio of L and M cones that was calculated from spectral sensitivity for L and M cones), and the background color with 23.0 and 11.5 cd/m^2 corresponds to equal energy white of 34.5 cd/m^2.

In order to measure the discrimination thresholds from each background, the test color was changed along one of eight directions between 0 and 180 degrees in the plane (45° interval). Note that the L + M direction here refers to the direction of 45° in the LM cone excitation coordinate, not the constant chromaticity direction that goes through the origin in the LM place (the achromatic direction or 45° in cone contrast space). Although the L + M direction is close to the achromatic direction, the thresholds do not have to be determined by the achromatic mechanism because of the spatiotemporal condition of stimulus used in Kawamoto *et al.*'s experiment. For model evaluation, however, we did not use the data of the L + M direction to avoid any possible influence of mechanisms other than the L – M opponent mechanism.

The stimulus was a 2 × 2 array of four 1° squares in a 6° × 6° square field with 0.1° black gaps separating the squares. The square colors and the background color were the same before the test stimulus presentation. The square can be visible due to the black gap. When the observer pressed a key, the color of one of the squares (test stimulus), chosen randomly for each trial, changed along one of the eight directions while the color of the other three squares was unchanged. The temporal profile of the test color change was a 1 Hz Gabor function with sine phase.

C. Procedure

In each trial, the test color was presented on one of the four squares selected randomly, with the other three squares remaining the same color as the background. The observer's task was to judge which of the four squares changed color. The test color was determined according to the predicted color distance from the background color using a staircase method (one up one down). The averages of the last five in the ten reversals were calculated as thresholds. Three observers with normal color vision participated in the experiment.

D. Results

Figure 1 shows the threshold data (squares) of all background colors (shown by crosses) in the LM plane. The horizontal and vertical axes represent L- and M-cone stimulus values in terms of luminance in cd/m^2. Each point represents the threshold from the corresponding background for one of four directions. In Fig. 1, we analyzed the results slightly differently

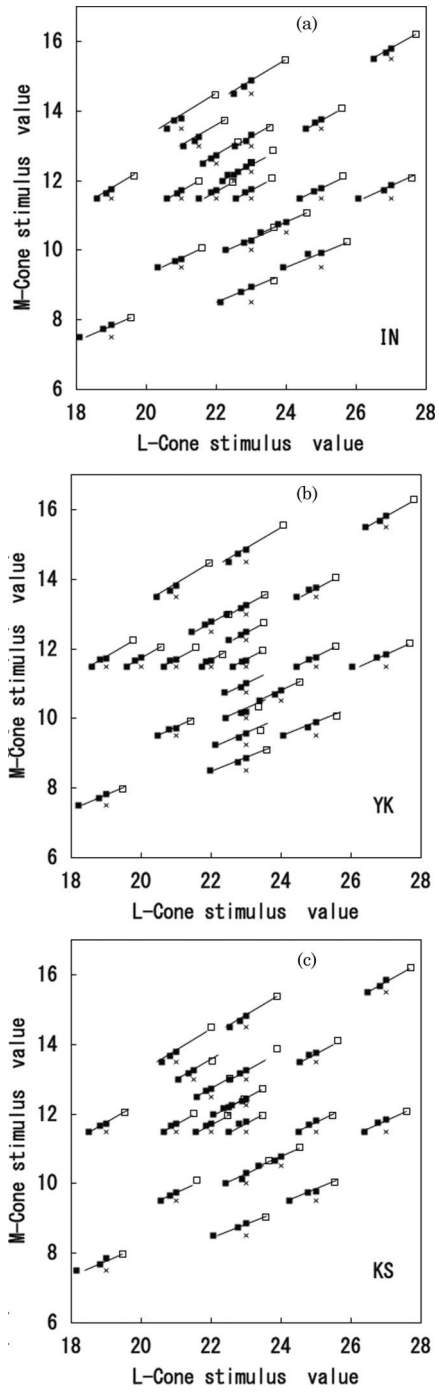

Fig. 1. Color discrimination thresholds of Kawamoto *et al.* [17] with model predictions. Each square indicates the color that is just discriminable from the color indicated by the cross (the background color). The open square is the one in the L + M direction, which is not used for modeling. The lines show the prediction of threshold (a), (b), (c) for observers IN, YK, and KS, respectively. Threshold values (distances from the background colors) are magnified by three times so that the results can be clearly seen.

from Kawamoto *et al.*, averaging the data from opposite test directions. This was because the color changes of the two test stimuli were the same (only the order of the color changes was different, e.g., gray–red–gray–green–gray versus gray–green–gray–red–gray) and also because the results were similar in the two cases (see Figs. 3 and 8 in Kawamoto *et al.* [17]) although thresholds were measured separately for two opposite test directions (e.g., 0 and 180°). Consequently, thresholds in four directions were obtained for each background color.

Model predictions are shown in Fig. 1 as lines together with experimental results (see Section 3 for model details). The lines suggest that the L – M mechanism determines the thresholds, including the L + M direction (open squares), with all background colors, because they are aligned along a line that is close to perpendicular to the L – M (135°) direction (though the slope varied from background to background).

Furthermore, data points plotted close to the prediction line up with all background for all of the three observers. This indicates that the model is capable of predicting the Kawamoto *et al.*'s results.

3. MODEL

Here, we describe Smith *et al.*'s [6] model with our modifications. The model assumed a gain control in the cones and an adaptation effect in the red–green color-opponent mechanism that responds nonlinearly (Fig. 2). The nonlinearities apply only for background colors. Difference in response between the test and background colors can be assumed to be linear since the difference is negligible relative to the response to the background color.

A. Cone Process

The gain controls of cone responses are formulated as follows (L cone in this example).

$$G(L) = \frac{1}{(1 + k_3 L)^{k_4}}, \qquad L = \frac{L_A}{l_{nor}}, \tag{1}$$

where L_A (or M_A in the case of M cone) is the cone activity in response to adaptation color (or background color in the experiment of Kawamoto *et al.*), l_{nor} (or m_{nor} in the case of M cone) is a parameter to normalize L (or M) cone responses, and k_3 and k_4 are constants that determine the function shape. In the present study, we determined l_{nor} and m_{nor} based on unique white measurement for each observer in Kawamoto *et al.* That is, we used cone responses to the unique white for each observer as l_{nor} and m_{nor}. This differs from the normalizing parameter of Smith *et al.*, who used the response to light at the peak sensitivity. The reason why we used the response to unique white (instead of peak sensitivity) for normalization is because unique white is invariant over a large range of stimulus intensities [23]. This invariance indicates that the excitations of the three cone classes maintain the same relative proportions as luminance varies, even with possible nonlinearity, and therefore all cone responses are expected to be equal at unique white [24]. We found that this modification of parameter values changed the model prediction only slightly in the data used here, but there could be large differences for much brighter stimuli.

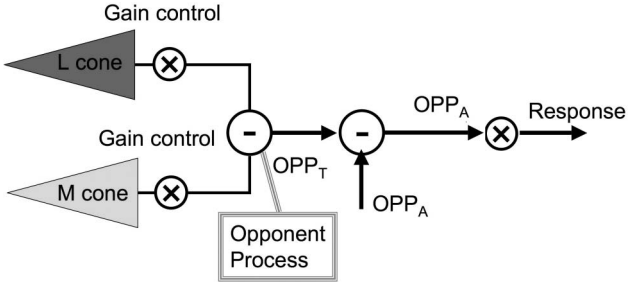

Fig. 2. Two-stage color vision model proposed by Smith *et al.* [6]. Cones have nonlinear outputs expressed by a gain control, and the opponent process output OPP also has a nonlinear output expressed by a Naka–Rushton type function. Adaptation to the background color is modeled by subtracting a certain percentage of the OPP activity in response to the background color (OPP_A). $OPP_{A'}$ represents the activity of the opponent mechanism after adapting to the background color.

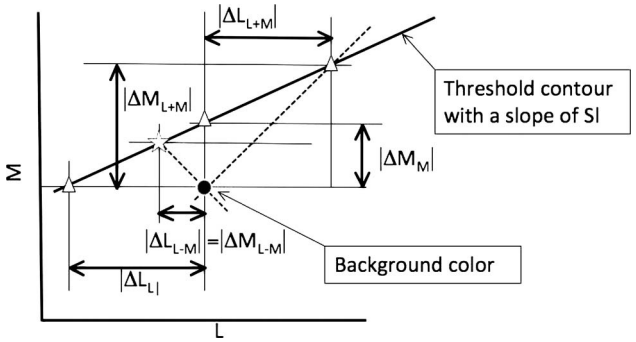

Fig. 3. Threshold contour that corresponds to the line expressed by Eq. (5). The thick solid line shows a threshold contour, which is determined by the threshold along the L – M direction (star) and a slope in Eq. (5). Threshold in other color directions [Eqs. (6)–(8)] are also shown (triangles).

B. Opponent Process

The red–green opponent signal, referred as L – M here, is formulated as the difference between L- and M-cone outputs for L-center and M-center opponent cells. The next equation describes the red–green mechanism with L cone center, which is assumed to be responsible for discrimination among reddish colors:

$$OPP_{(+LWS-MWS)} = \frac{L_T}{l_{nor}} G(L_A/l_{nor}) - k_2 \frac{M_T}{m_{nor}} G(M_A/m_{nor}), \tag{2}$$

where L_T and M_T are cone activity in response to the test color, and k_2 is a parameter that determines the contribution of the signal from the receptive field surround. We adopted the same values as in Smith *et al.*'s study for k_3 and k_4, but we used 1.0 for k_2 instead of their 0.8, which was based on physiological data. This was because any value of k_2 except 1.0 changes the contribution ratio of L and M cones to the L-center and M-center opponent cells, making it difficult to predict the results of Kawamoto *et al.* (see Section 4).

The sensitivity change caused by color adaptation is modeled as in the following equation:

$$OPP_{A'} = (1 - k_1) \cdot OPP_A, \tag{3}$$

where OPP_A represents the activity of the opponent mechanism in response to the background color and $OPP_{A'}$ represents the activity of the opponent mechanism after adapting to the background color. The parameter k_1 represents the

Table 1. Fitting Parameters and Coefficients of Determination (R^2) for the Present Model, SPS Model, and the Present Model with Variable k_1 [a]

	Present Model			SPS Model			Variable k_1
Without L + M	Subject IN	Subject YK	Subject KS	Subject IN	Subject YK	Subject KS	Subject IN
δ/R_{max}	0.323	0.312	0.238	0.035	0.002	0.061	0.041
SAT	0.084	0.089	0.121	0.02	0.001	0.061	0.028
R^2	0.923 (0.060)	0.913(0.116)	0.935(0.062)	0.739(0.235)	0.813(0.166)	0.839(0.219)	0.945(0.050)
	Present Model			SPS Model			Variable k_1
With L + M	Subject IN	Subject YK	Subject KS	Subject IN	Subject YK	Subject KS	Subject IN
δ/R_{max}	0.301	0.282	0.223	0.039	0.006	0.061	0.039
SAT	0.098	0.105	0.137	0.021	0.003	0.052	0.041
R^2	0.965(0.022)	0.943(0.094)	0.962(0.032)	0.861(0.096)	0.846(0.143)	0.894(0.105)	0.968 (0.024)
k_1		0.9			0.9		varied
k_2		1			0.8		1
k_3		0.33			0.33		0.33
k_4		0.75			0.75		0.75

[a]Fitting without and with thresholds in the L + M direction.

strength of subtractive feedback. Perfect adaptation ($k_1 = 1$) predicts no effect of background color because the $OPP_{A'} = 0$ indicates that the response of the opponent process to any background color is the same as that to the neutral white. We adopted k_1 of 0.9, following Smith *et al.* The next equation shows the nonlinear output, R, of the opponent response, OPP:

$$R = R_{\max} \cdot \frac{\mathrm{OPP}}{\mathrm{OPP} + \mathrm{SAT}}, \tag{4}$$

where R_{max} is the maximum response and SAT is the half-saturation index.

C. Discrimination Threshold

The threshold contour for color discrimination with each adaptation is expressed as below (see the details in Appendix A). Since the model assumes that the difference between the test and background colors is linearly related to the neural response, the threshold contour becomes a line. Here, we derived the threshold contour line from Eqs. (1)–(4) and show it by the threshold ΔL along the L – M axis ($|\Delta L_{L-M}| = |\Delta M_{L-M}|$) with its slope (Sl) in the next equation:

$$\Delta L_{L-M} = \frac{\Delta\mathrm{OPP}}{\frac{G(L)}{l_{\mathrm{nor}}} + \frac{G(M)}{m_{\mathrm{nor}}}}, \qquad \mathrm{Sl} = G(L)/G(M),$$

$$\text{where } \Delta\mathrm{OPP} = \frac{\delta}{R_{\max}} \cdot \frac{(\mathrm{OPP}_{A'} + \mathrm{SAT})^2}{\mathrm{SAT}} \quad \text{and}$$

$$L = \frac{L_A}{l_{\mathrm{nor}}}, \qquad M = \frac{M_A}{m_{\mathrm{nor}}}, \tag{5}$$

where δ represents the activation difference at threshold. Although Eq. (5) is sufficient to represent a threshold contour, an explicit expression is required for threshold of each test color direction in order to perform least-square fitting. For the purpose, we need slightly different equations, considering the relationship between ΔM and ΔL that is specific to each color direction. The thresholds along the L, M and L + M directions (ΔL_L, ΔM_M and ΔL_{L+M}) are formulated as follows (see Fig. 3):

$$\Delta L_L = \frac{\Delta\mathrm{OPP}}{\frac{G(L)}{l_{\mathrm{nor}}}}, \tag{6}$$

$$\Delta M_M = \frac{\Delta\mathrm{OPP}}{\frac{G(M)}{m_{\mathrm{nor}}}}, \tag{7}$$

$$\Delta L_{L+M} = \frac{\Delta\mathrm{OPP}}{\frac{G(L)}{l_{\mathrm{nor}}} - \frac{G(M)}{m_{\mathrm{nor}}}}. \tag{8}$$

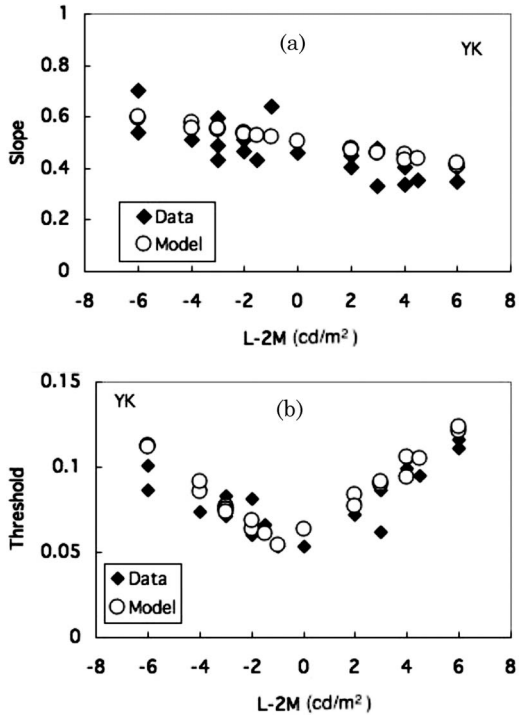

Fig. 4. (a) Slope of the threshold contour as a function of L – 2M value (activity of opponent color). Open circles represent model prediction, and solid diamonds represent the slope of the line fitted to experimental results (YK). (b) Threshold expressed by the distance of the threshold contour from the background color. The data are again shown as a function of L – 2M.

ΔL_{L-M}, ΔL_L, ΔM_M, and ΔL_{L+M} of Eqs. (5)–(8) are fitted to experimental data for each observer using a least-square method. In the method, we used only two free parameters, δ/R_{max} and SAT, which were common for all background conditions.

D. Prediction

The lines near the data plots in Fig. 1 show the model predictions, and Table 1 shows the fitting parameters and the coefficients of determination. The fitting parameters with inclusion of the L + M direction data are also shown as a record. For three observers, the fitting parameters δ/R_{max} and SAT varied between 0.238 and 0.323 and between 0.084 and 0.121. The coefficients of determination are larger than 0.9 on average for all observers.

The model predicts that the changes both in distance of the threshold contours from the background and in slope of the threshold contour are dependent on background or adaptation colors. Two factors are shown separately in panels in Figs. 4(a) and 4(b) as a function of L – 2M of background color. The value of L – 2M corresponds to the horizontal axis of the MacLeod–Boynton chromaticity coordinates, where the value of the equal energy white is zero. Figure 4(a) shows that the slope of the threshold contour decreases monotonically with an increase of L – 2M both in the data and in the prediction. Figure 4(b) shows the discrimination threshold, which is defined as the distance of the line fitted to the three data points from the background color. The threshold is lowest at about zero of L – 2M, which corresponds to the neutral point of the red–green opponent channel, both in the data and in the prediction. These results confirm the validity of the model for color discrimination with luminance variation.

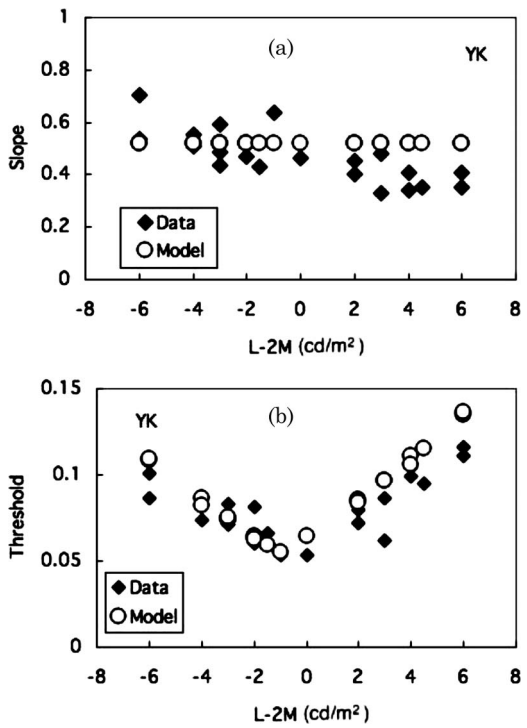

Fig. 5. Model prediction of (a) slope and (b) threshold but without nonlinearity of the cone process. Experimental results are from YK.

E. Nonlinearity

Next, we examined whether nonlinearity at the two stages is necessary to explain the experimental data. Although the model assumed nonlinear responses both in the cone and opponent processes based on physiological evidence, it is not clear whether nonlinearity at both stages is necessary or whether nonlinearity at either stage is sufficient to interpret psychophysical data in the model. We manipulated the model parameters to investigate this question. The analysis revealed that nonlinearity is necessary at both of the stages. Importantly, nonlinearities at the two stages show different effects on color adaptation. The analysis showed that a nonlinear response at the cone stage is required to explain the slope change in threshold contours and that a nonlinear response at the opponent process is required for threshold change depending on the adaptation state. When a linear function is used for cone responses [i.e., G(L) = 1], the threshold is expected to change dependent on background colors because of the nonlinearity of the opponent process. Figure 5 shows the prediction with linear cone responses. The threshold changes that are dependent on the background color can be predicted with an accuracy similar to the original prediction with nonlinear cone responses [Fig. 5(b)]. However, the prediction shows a constant slope of the threshold contour across opponent responses to background color, which is inconsistent with the experimental results.

On the other hand, when a linear function is used for the opponent response (i.e., R = OPP) with gain control of cone responses, the slope of the threshold contour decreases with an increase in opponent response to background color [Fig. 6(a)], as does the experimental result. However, the prediction does not show a V-shaped function for threshold [Fig. 6(b)], which is an important feature of the experimental

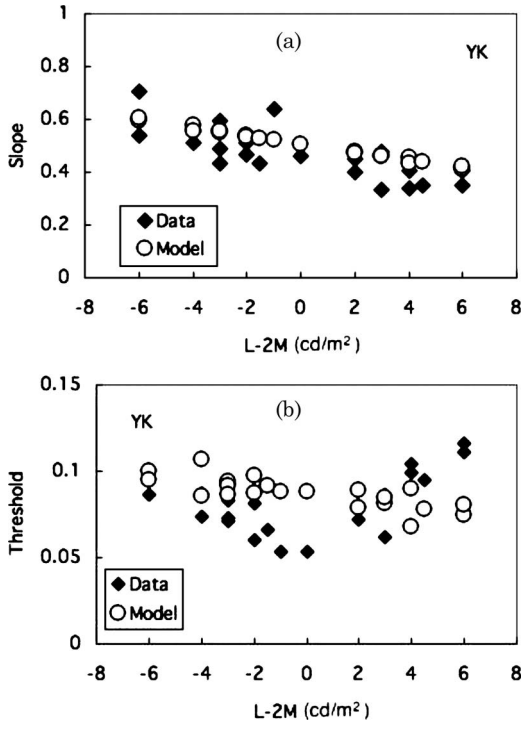

Fig. 6. Model prediction of (a) slope and (b) threshold but without nonlinearity of the opponent process. Experimental results are from YK.

results. The analysis revealed that nonlinearity at both cone and opponent processes contributes to color discrimination thresholds, while the manner of contribution is different.

F. Comparison with the SPS Model

We compared the present model with the original SPS model. A few parameters were different from the SPS model as described in Subsections 3.A and 3.B, and the comparison of model predictions revealed how the differences influence the prediction of color discrimination thresholds.

The fitting parameters and coefficients of determination are shown in Table 1 for each model. Figure 7 compares the predictions in five backgrounds as representatives: the lightest, darkest, and two extreme saturated color backgrounds among isoluminance backgrounds (the highest L response and highest M response backgrounds), and the neutral background. The present model showed a better prediction than the SPS model in terms of least-square fitting. Particularly, the present model predicted slopes better than the SPS model. Results for the other observers are similar (not shown) as coefficients of determination suggest (Table 1). The coefficients of determination shown are averages over different background colors. A paired t-test showed that the difference in coefficients of determination between the present and the SPS models is statistically significant for the three observers ($t = 3.41$, $p < 0.01$ for IN; $t = 2.59$, $p < 0.05$ for YK; $t = 2.33$, $p < 0.05$ for KS). We used a paired t-test here for the data from the same background colors, because the coefficient of determination tends to vary dependently on the background. The small but significant improvement in the present model should be attributed to the modifications described in Subsections 3.A and 3.B, and it suggests importance of the modifications.

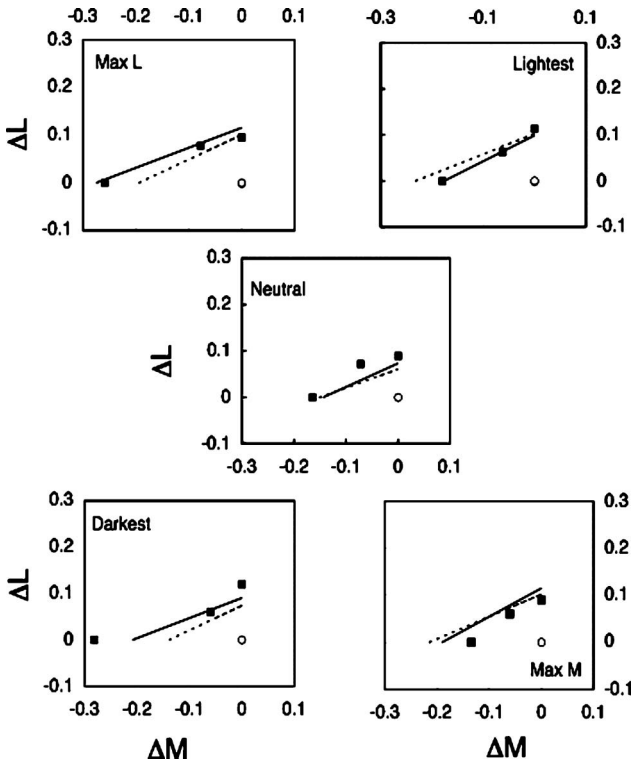

Fig. 7. Comparison of model predictions for five background colors. The solid line and the dashed line in each panel indicate the prediction of the present model and that of SPS model, respectively. Solid squares represent experimental results (KS). Units are cd/m^2 as in Fig. 1.

G. Analysis with the Data along the L + M Direction

We repeated the analysis with the results in the L + M color direction. Although there might be influence of other mechanisms such as luminance or yellow–blue [or S – (L + M)] mechanisms, Fig. 1 suggests that the threshold in the L + M direction is determined by the same mechanism that determines threshold in other directions, which we assume is the L – M color-opponent mechanism. Including the data in the L + M direction potentially increases data precision and model estimation. Fitting parameters and coefficients of determination obtained with the data are shown in Table 1. The parameters are similar to, and the coefficients of determination are slightly larger than, those without the data of the L + M direction. The same paired t-test as in the original analysis showed that the difference in coefficients of determination between the present and the SPS models is statistically significant for the three observers ($t = 5.26$, $p < 0.01$ for IN; $t = 3.67$, $p < 0.01$ for YK; $t = 3.66$, $p < 0.01$ for KS).

4. DISCUSSION

We extended the color discrimination model proposed by Smith *et al.* to color discrimination results with luminance changes. Our analysis showed that the model predicts color discrimination thresholds for a variety of test colors on a variety of background colors on the LM plane. A detailed analysis of the model predictions revealed that nonlinearity at both cone and opponent stages is necessary to explain the data. The nonlinearity at each stage influences the discrimination threshold differently. This is consistent with notion of the difference in color discrimination thresholds among different background colors found even in cone contrast space (e.g., [7,10]). If one assumes that the cone stage has logarithmic nonlinearity as predicted from Weber-like adaptation, the difference in threshold in cone contrast space should be attributed to the influence of the second (or later) stage such as the L – M mechanism. The present study elaborates two-stage models of color vision, considering the nonlinearity at both stages.

In this section we discuss the influence of the parameters k_1 and k_2 in the model with additional analyses and a supplemental experiment. The parameter k_1 represents the degree of adaptation of the red–green opponent mechanism to the background color, and the parameter k_2 represents the strength of the signal from the receptive field surround relative to that from the receptive field center. We adopted the same value of k_1 for all background color conditions in the model prediction above, following the SPS model. However, it is likely that adaptation-state changes are dependent on the background color. For example, Kuriki and Uchikawa measured the color coordinates of unique white under a variety of illumination conditions [25]. They analyzed the results in terms of relative sensitivity changes among L, M, and S cones and found that the degree of sensitivity change estimated from the data is smaller than that required for color constancy predicted from the von Kries model. If color constancy is perfect, the color of illumination light or that of white paper will be perceived as white under any illumination. In such a situation, the unique white should have the same color coordinates as those of the

illumination. However, the measured unique white was somewhere between equal energy white and the illumination color in CIE xy color coordinates, as is commonly found in studies in the field. Cone sensitivity changes with various illuminations, but the change is usually less than that for perfect constancy.

We tried modeling with different k_1 values for different backgrounds, taking account of the adaptation state in each condition. These k_1 values were obtained from a fitting parameter that expressed linear reduction of k_1 with distance from the unique white point along the L – 2M axis. The point of unique white was the point measured psychophysically in Kawamoto *et al.* with a color naming procedure, and the value of k_1 was fixed as 1.0 for the color. With this modification, the root-mean-square error decreased by 3% compared with the original model (slight increase in R^2 as shown in Table 1), which used the fixed k_1 of 1.0 for all background colors. This suggests potential importance of the change of k_1 dependent on background colors.

Moreover, we found that the value of k_1 for each background color was related to the actual adaptation state in a supplemental experiment. In the experiment, we measured the color that provides perception of unique yellow (red–green equilibrium) for each background color. The task was to obtain the red–green equilibrium in the test field by varying the red/green ratio of the test color along the L – M direction with a constant luminance. The observer adjusted the color so that it appeared to be unique yellow (or white if neither yellow nor blue was seen in the test). If adaptation is perfect, the background color should appear unique yellow (or white) and the observer should set the test color for unique yellow so that the L – 2M value of the color is the same as that of the background color (which corresponds to $k_1 = 1.0$). Based on the ratio between the L – 2M value for unique yellow and the value for background color, an appropriate value of k_1 was obtained experimentally under each condition. The stimulus was the same as the color in the discrimination experiment, and the color in all squares of the test field was varied by one of the authors, IN.

Figure 8 compares k_1 estimated from the experiment and the value obtained from the model parameters, predicting the color discrimination results in terms of least-square errors. The results show that adaptation was nearly complete when the L – 2M value of the background color was close to zero, but the degree of adaptation (or k_1) decreased as the absolute of the L – 2M of background color increased (i.e., became more saturated). The comparison showed that the two different methods provided similar estimates of k_1 for all background colors. It is also interesting that the decrease in k_1 was not symmetric to background colors; it decreased slightly on the green background, whereas it decreased drastically on the red background, suggesting that the adaptation was less complete on the red background. This asymmetry of the color at the second site could be associated with results of Chaparro *et al.* [16]. They measured threshold contours in red, yellow, and green backgrounds for detection of the test stimuli modulating L- and M-cone contrast space. They found that the sensitivity of the L – M chromatic mechanism at the second site decreased on the red background relative to those in yellow and green backgrounds. Subsequently, Eskew *et al.* proposed a model considering the second-site effect (or "second-site desensitization") [7]. Although no truly satisfactory explanation of the asymmetry at the second site has been found, it seems that such asymmetry could be considered for color discrimination model in the future research.

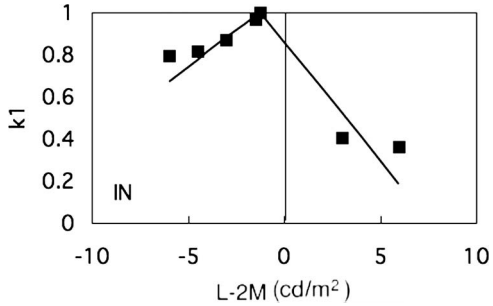

Fig. 8. Parameter k_1 estimated from unique yellow measurements (squares) and model predictions (line).

Next, we consider the effect of parameter k_2. In Eq. (2) we assumed parameter k_2 equals 1.0, whereas Smith *et al.* used a k_2 value of 0.8 based on physiological results. Here we show how differences in the parameter influence the prediction of color discrimination results. Figure 9 shows the slope of threshold contours from predictions with $k_2 = 0.8$ [compare with Fig. 4(a), which is the same prediction but with $k_2 = 1.0$]. Unlike the prediction in Fig. 4(a), here the slope changes rather abruptly at the unique white point. This is caused by the difference in the ratio of contribution of the L and M cones to the opponent channel between the red and green sides of the unique white. The model assumes that L-center cells determine the threshold when L – 2M is positive and that M-center cells determine the threshold when L – 2M is negative (the present model classified conditions into two groups based on the value of L – 2M for unique white measured for each observer). As with $k_2 = 0.8$, the difference in contribution between center and surround signals of the receptive field causes discontinuity of the cone ratio at the unique white point.

The above discussion on the effect of k_2 suggests that there is a discrepancy between the physiological and psychophysical estimates of the ratio of the center and surround signals in the receptive field of color-opponent cells. Although we cannot address this issue directly because we do not know how the outputs of a cell are related to psychophysical responses, it may be possible to interpret the difference in terms of the effect of the integration processes of physiological units. A human observer makes decisions based on the responses of many cells. There may be an integration process that

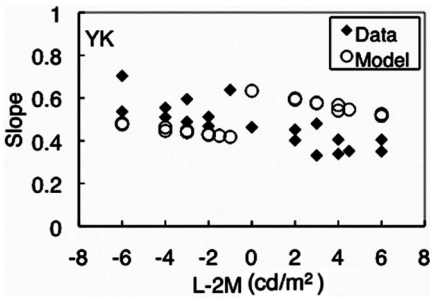

Fig. 9. The open circle indicates the threshold contour slope predicted by the model with 0.8 of k_2, which value was used in Smith *et al.* The solid diamond shows the experimental results [YK as in Fig. 4(a)].

subtracts signals from the two types of cells like those assumed in double-opponent cells [26]. Such a process perhaps compensates for the difference in ratio of contribution of L and M cones to the opponent process. The relative weights of L- and M-cone responses to double opponent cells are balanced, because both L- and M-cone signals come from the receptive field center as from the receptive field surround. No asymmetry in the cone contribution remains between the L-center and M-center mechanisms in psychophysical results in such cases.

In conclusion, we applied the color vision model proposed by Smith *et al.* to predict color discrimination thresholds with various background colors and several test directions on the LM plane. With appropriate modifications, the model predicted the empirical results successfully. In addition, the model showed different influence of nonlinearity in the cone and cone-opponent stages both in qualitatively and quantitatively.

APPENDIX A

In order to obtain the equation for threshold contours, we solved Eq. (4) by ΔL or ΔM with a constraint from each color change direction (Fig. 3). Since test color does not influence Eqs. (3) and (4), the OPP at threshold ΔOPP can be expressed by response R at threshold δ as follows:

$$\begin{aligned} \frac{\delta}{\Delta\mathrm{OPP}} \cong \frac{dR}{d\mathrm{OPP}} &= R_{\max} \cdot \frac{\mathrm{SAT}}{(\mathrm{OPP}_{A'} + \mathrm{SAT})^2}, \\ \Delta\mathrm{OPP} &= \frac{\delta}{R_{\max}} \cdot \frac{(\mathrm{OPP}_{A'} + \mathrm{SAT})^2}{\mathrm{SAT}}. \end{aligned} \tag{A1}$$

In the case of the L – M direction, ΔL is obtained as in Eq. (5) (where $k_2 = 1.0$) by solving the following simultaneous equations:

$$\begin{cases} \Delta\mathrm{OPP} = \frac{\Delta L}{l_{\mathrm{nor}}} G(L_A/l_{\mathrm{nor}}) - \mathrm{k}_2 \frac{\Delta M}{m_{\mathrm{nor}}} G(M_A/m_{\mathrm{nor}}) \\ \Delta L + \Delta M = 0 \end{cases}. \tag{A2}$$

The first equation in (A2) is derived from Eq. (2) assuming that the gain is determined solely by background color as follows:

$$\begin{aligned} \Delta\mathrm{OPP} &= \mathrm{OPP}_t - \mathrm{OPP}_A \\ &= \frac{(L_A + \Delta L)}{l_{\mathrm{nor}}} G(L_A/l_{\mathrm{nor}}) - \mathrm{k}_2 \frac{(M_A + \Delta M)}{m_{\mathrm{nor}}} G(M_A/m_{\mathrm{nor}}) \\ &\quad - \left(\frac{L_A}{l_{\mathrm{nor}}} G(L_A/l_{\mathrm{nor}}) - \mathrm{k}_2 \frac{M_A}{m_{\mathrm{nor}}} G(M_A/m_{\mathrm{nor}}) \right) \\ &= \frac{\Delta L}{l_{\mathrm{nor}}} G(L_A/l_{\mathrm{nor}}) - \mathrm{k}_2 \frac{\Delta M}{m_{\mathrm{nor}}} G(M_A/m_{\mathrm{nor}}). \end{aligned} \tag{A3}$$

For the color directions of L, M, and L + M, the equation ΔL + ΔM = 0 is replaced by ΔM = 0, ΔL = 0, and ΔL – ΔM = 0; and the simultaneous equations are solved by ΔL, ΔM, and ΔL; and the results are shown in Eqs. (6)–(8).

ACKNOWLEDGMENTS

This study is partially supported by the Ministry of Education, Science, Sports, and Culture of Japan (MESSC-JP), KAKENHI (Grants-in-Aid for Scientific Research) (B) 22330198 (2010) to S. Shioiri, and the Cooperative Research Project of the Research Institute of Electrical Communication (RIEC) at Tohoku University.

REFERENCES

1. G. Wyszecki and W. S. Stiles, *Color Science: Concepts and Methods, Quantitative Data and Formulas*, 2nd ed. (Wiley, 1982).
2. D. L. MacAdam, "Visual sensitivities to color differences in daylight," J. Opt. Soc. Am. **32**, 247–274 (1942).
3. R. M. Boynton, A. L. Nagy, and C. X. Olson, "A flaw in equations for predicting chromatic differences," Color Res. Appl. **8**, 69–74 (1983).
4. G. R. Cole, T. H. Hine, and W. McIlhagga, "Detection mechanism in L-, M- and S-cone contrast space," J. Opt. Soc. Am. A **10**, 38–51 (1993).
5. S. L. Guth, "Model for color vision and light adaptation," J. Opt. Soc. Am. A **8**, 976–993 (1991).
6. V. C. Smith, J. Pokorny, and V. C. Sun, "Chromatic contrast discrimination: data and prediction for stimuli varying in L and M cone excitation," Color Res. Appl. **25**, 105–115 (2000).
7. R. T. Eskew, Jr., J. S. McLellan, and F. Giulianini, "Chromatic detection and discrimination," in *Color Vision: From Genes to Perception*, K. Gegenfurtner and L. T. Sharpe, eds. (Cambridge University, 1999), pp. 345–368.
8. J. E. Thornton and E. N. Pugh, Jr., "Red/green color opponency at detection threshold," Science **219**, 191–193 (1983).
9. G. R. Cole, T. J. Hine, and W. McIlhagga, "Estimation of linear detection mechanisms for stimuli of medium spatial frequency," Vis. Res. **34**, 1267–1278 (1994).
10. R. T. Eskew, Jr., C. F. Stromeyer, III, and R. E. Kronauer, "Temporal properties of the red–green chromatic mechanism," Vis. Res. **34**, 3127–3137 (1994).
11. M. Ikeda and M. Urakubo, "Flicker HTRF as test of color vision," J. Opt. Soc. Am. **58**, 27–31 (1968).
12. C. F. Stromeyer, III, G. R. Cole, and R. E. Kronauer, "Second-site adaptation in the red–green chromatic pathways," Vis. Res. **25**, 219–237 (1985).
13. A. Eisner and D. I. Macleod, "Flicker photometric study of chromatic adaption: selective suppression of cone inputs by colored backgrounds," J. Opt. Soc. Am. **71**, 705–717 (1981).
14. M. J. Sankeralli and K. T. Mullen, "Postreceptoral chromatic detection mechanisms revealed by noise masking in three-dimensional cone contrast space," J. Opt. Soc. Am. A **14**, 2633–2646 (1997).
15. K. R. Gegenfurtner and D. C. Kiper, "Contrast detection in luminance and chromatic noise," J. Opt. Soc. Am. A **9**, 1880–1888 (1992).
16. A. Chaparro, C. F. Stromeyer, III, G. Chen, and R. E. Kronauer, "Human cones appear to adapt at low light levels: measurements on the red–green detection mechanism," Vis. Res. **35**, 3103–3118 (1995).
17. K. Kawamoto, T. Inamura, H. Yaguchi, and S. Shioiri, "Color discrimination characteristics depending on the background color in the (L, M) plane of a cone space," Opt. Rev. **10**, 391–397 (2003).
18. C. F. Stromeyer, III, P. D. Gowdy, A. Chaparro, S. Kladakis, J. D. Willen, and R. E. Kronauer, "Colour adaptation modifies the temporal properties of the long- and middle-wave cone signals in the human luminance mechanism," J. Physiol. **526**, 177–194 (2000).
19. C. F. Stromeyer, III, R. Thabet, A. Chaparro, and R. E. Kronauer, "Spatial masking does not reveal mechanisms selective to combined luminance and red–green color," Vis. Res. **39**, 2099–2112 (1999).
20. S. Tsujimura, S. Shioiri, and A. Nuruki, "Two distinct cone-opponent processes in the L + M luminance pathway," Vis. Res. **47**, 1839–1854 (2007).
21. S. Tsujimura, S. Shioiri, Y. Hirai, and H. Yaguchi, "Technique to investigate the temporal phase shift between L- and M-cone inputs to the luminance mechanism," J. Opt. Soc. Am. A **17**, 846–857 (2000).
22. S. Tsujimura, S. Shioiri, Y. Hirai, and H. Yaguchi, "Selective cone suppression by the L – M- and M – L-cone-opponent mechanisms in the luminance pathway," J. Opt. Soc. Am. A **16**, 1217–1228 (1999).

23. J. Walraven and J. S. Werner, "The invariance of unique white; a possible implication for normalizing cone action spectra," Vis. Res. **31**, 2185–2193 (1991).
24. S. Shioiri and P. Cavanagh, "Nonlinearity in color space measured by apparent motion," Percept. Psychophys. **62**, 1182–1190 (2000).
25. I. Kuriki and K. Uchikawa, "Adaptive shift of visual sensitivity balance under ambient illuminant change," J. Opt. Soc. Am. A **15**, 2263–2274 (1998).
26. B. R. Conway and M. S. Livingstone, "Spatial and temporal properties of cone signals in alert macaque primary visual cortex," J. Neurosci. **26**, 10826–10846 (2006).